Int. J. Nano Dimens., 9 (2): 145-157, Spring 2018

ORIGINAL ARTICLE

CuO nano structures as an ecofriendly nano photo catalyst and antimicrobial agent for environmental remediation

***Asha Radhakrishnan*[*1]; *Padmavathi Rejani*[2]; *Bhaskaran Beena*[3]**

[1]*Department of Chemistry Devaswam Board Pampa College, Parumala, Pathanamthitta, Kerala, PIN 689626, India*
[2]*Nano Science Research Lab, Department of Chemistry, D. B. College, Sasthamcotta, Kollam, Kerala, India*
[3]*Nanoscience Research Lab, Department of Chemistry Devaswom Board College Sasthamcotta, Kollam, Kerala, PIN 690522, India*

Received 23 September 2017; revised 21 December 2017; accepted 01 February 2018; available online 03 February 2018

Abstract

Present work focuses on the synthesis strategies for different CuO nanostructures along with associated formation mechanisms and their interesting fundamental properties, and promising applications in biological and environmental remediation. We present a variety of synthesis techniques for producing diverse types of CuO nanostructures with various morphologies such as nanoparticles, nanoleaves, nanotubes, and nanoflowers. The effect of synthesis parameters on manipulating the nanoscale features along with the associated growth mechanisms for these unique morphologies is also discussed. The surface, electronic and optical properties of these nanostructures is also detailed. The photocatalytic and antimicrobial applications of these nanostructures are systematically introduced and summarized. Congo red and Malachite green organic dyes were degraded by these CuO nanostructures and it was found that CuO nanoflowers are more favorable for the degradation of Congo red and Malachite Green due to their higher surface sites and surface defects. Overall, in addition to size, morphology has a significant effect on the properties and applications of nanomaterials. The synthesized novel hierarchical CuO nanostructures with large surface areas and carefully defined surfaces are best suited for treating industrial effluents.

Keywords: *Antimicrobial activity; Biogenic method; CuO nanostructures; Nano photocatalyst; Photodegradation.*

How to cite this article

Radhakrishnan A, Rejani P, Beena B. CuO nano structures as an ecofriendly nano photo catalyst and antimicrobial agent for environmental remediation. Int. J. Nano Dimens., 2018; 9 (2): 145-157.

INTRODUCTION

Copper oxide has been a hot topic among the studies on transition metal oxides because of its interesting properties. CuO nanostructures with the large surface area and size effects possess superior physical and chemical properties that remarkably different from those of their bulk counterparts [1, 2]. CuO nanostructures are extensively used in various applications including gas sensors [3], biosensors [4], nanofluid [5], photodetectors [6], supercapacitors [7], removal of inorganic pollutants and photocatalysis [8] because of their simplicity of preparation, scalability, non-toxicity, abundance, low-cost, and environmental friendliness [9]. The superhydrophobic properties of CuO nanostructures render these materials as promising candidates in Lotus effect self-cleaning coatings (anti-biofouling), surface protection, textiles, water movement, microfluidics, and oil–water separation.

Various efforts have been focused on the fabrication of nanostructures to improve their performance in currently existing applications [10]. Since the properties of CuO can be greatly affected by morphologies, intense research has been focused on the controlled preparation of various CuO nanostructures over the last two decades. However, it is still a great challenge to achieve high-rate capability and crystallinity in nanostructures. It is well recognized that a smaller size of CuO can

* Corresponding Author Email: *ashagopan2009@gmail.com*

lead to higher capacity and higher rate capability. Therefore, the synthesis of CuO nanostructures with ultrafine size is a promising approach to obtain large-surface area and high-aspect-ratio. In the present study, CuO nanostructures have been synthesized by a biogenic method using the juice of pomegranate (pg), characterized by its high phenolic content and antioxidant properties. The synthesized nanostructures were characterized by X-ray diffraction, Scanning electron microscopy, Transmission electron microscopy, Fourier Transform Infrared Spectroscopy, Photoluminescence and UV- Visible absorption spectroscopy. The evaluations of the photocatalytic efficiency of these materials were carried out using the degradation of two organic dyes namely Malachite green and Congo Red. Further, these materials were tested for their antimicrobial properties against bacterial and fungal strains.

EXPERIMENTAL

Materials and methods

Cu $(CH_3COO)_2.H_2O$ was procured from Sigma Aldrich. All the solutions for the synthesis of Copper Oxide were freshly prepared using demineralized water.

Synthesis of CuO nanoparticles,

100mL of 0.1M copper acetate ($Cu(CH_3COO)_2.H_2O$) was taken in a 400 mL beaker to which 100mL of 1M NaOH solution and 20 mL of Pomegranate fruit extract (pg) were added simultaneously with constant stirring for 2 hours. The slurry obtained was kept for 24 hours in a hot air oven. The final product was washed, dried and calcinated at 100 ^{0}C to get the CuO nanoparticles.

Preparation Of CuO nanotubes

For the preparation of CuO nanotubes, 0.25 gm of Copper acetate was dissolved in 65ml of pg juice extract to which an appropriate quantity of a moderate alkali namely hexamethylenetetramine $\{(CH_2)_6N_4\}$, HMT} was added so as to attain a P^H level of 7. The resulting solution was then stirred well for 30min to obtain a homogeneously turbid liquid, which was then irradiated by a 300W domestic microwave oven for 20 min. The precipitate obtained was then cooled to room temperature, filtered, washed with distilled water followed by drying in a hot air oven at 90^{0}C for 24 hours.

Preparation of CuO nanoflowers and nanoleaves

For the synthesis of flowers and leaves like CuO nanostructures, microwave assisted method was used in which 100 mL aqueous solution of copper acetate (0.1 M), 150 mL of HMT (1 mM) and 22.7 mL of pg juice were mixed and stirred for half an hour. Then the solution was irradiated by a 300W domestic microwave oven for 30 min. The reaction vessel was then kept in a laboratory oven at 90 ^{0}C for 5hours for growing the CuO nanoflowers. After the growth of CuO flowers, the slurry was washed with water and left to dry at room temperature. However, for the growth of CuO nanoleaves, 10mL of NaOH (1M) was also added to the aqueous solution of copper acetate and HMT before irradiation.

Characterization of samples

The synthesized samples of nano CuO were well characterized by instrumental techniques like SEM, TEM, FTIR, PL and UV-Visible spectroscopic studies.

In the present study, the prepared nano CuO samples were used as photocatalysts for the degradation of two organic dyes namely Congo red (CR) and Malachite green (MG).The degradation of the dyes MG and CR were followed by measuring the absorbance using a JASCO V 650, UV-Visible spectrophotometer. The degradation experiments were performed with a homemade photoreactor equipped with three 18W UV lamps with a wavelength of 254nm. The degradation efficiency of the prepared catalysts was optimized by varying experimental parameters such as pH, the concentration of dyes and weight of the catalyst taken. In a typical experiment, the photocatalyst was mixed with 300 mL of the dye solution and stirred in the dark for 30 min to establish an adsorption/ desorption equilibrium. After UV irradiation for the specific period of time, the dye concentration was determined by measuring the absorbance.

Acidic dye Congo red and basic dye Malachite green of 1000 ppm concentration were prepared and the desired concentrations were obtained by dilution.

The photocatalytic degradation efficiency was calculated as follows:

$$Removal\ (R\%) = \frac{(C_0 - C_t)}{C_0} \times 100 \quad (1)$$

C_0: initial concentration of dye solution [mgL^{-1}],
C_t: final concentration of dye solution [mgL^{-1}],

The antibacterial activity of nano CuO against pathogenic microbial species like *Escherichia coli, Pseudomonas aeruginosa, Bacillus subtilis and Streptococcus aureus* were evaluated by modified Kirby-Bauer disc diffusion method. The pure cultures of organisms were subcultured in Müller-Hinton broth at 35 °C ± 2 °C on an orbital shaking incubator at 160 rpm. For microbial growth, a lawn of culture was prepared by spreading the 100 µL fresh culture having 106 colony-forming units (CFU)/mL of each test organism on nutrient agar plates with the help of a sterile glass-rod spreader. Plates were left standing for 10 minutes to let the culture get absorbed. Than 8 mm wells were punched into the nutrient agar plates for testing nanomaterial antimicrobial activity. Wells was sealed with one drop of molten agar (0.8% agar) to prevent leakage of nanomaterials from the bottom of the wells. Using a micropipette, 100 µL (50 µg) of the sample of nanoparticle suspension was poured onto each of wells on all plates. After overnight incubation at 35 °C ± 2 °C, the different levels of the zone of inhibition were measured around the disc in units of a millimeter. Discs soaked in pure solvent, dimethyl sulfoxide (DMS) were used as a control.

RESULTS AND DISCUSSION

Physical appearance and stability

All the CuO nanostructures were obtained as black crystalline powders. The materials were found to be stable in mineral acids like H_2SO_4,HCl, HNO_3 in bases like NaOH and KOH at all concentrations as evidenced by no change in colour, form or weight of the sample used. They were also found to be stable in organic solvents like ethanol, acetone, glacial acetic acid, diethyl ether, methyl acetate, hexane etc.

XRD analysis

The XRD patterns of CuO nanostructures are well matched with the monoclinic phase of CuO (tenorite) and well consistent with the standard data reported by JCPDS (card no: 89-2531). Fig. 1 shows the XRD spectrum of CuO (a) nanoparticles (b) nano leaves (c) nanotubes and (d) nanoflowers. The sharp peaks and line widths of these diffraction peaks indicate that all the CuO nanostructures are crystalline. The average crystallite size calculated using Scherrer formula for the synthesized CuO nanoparticles, nanotubes, nanoflowers and nano leaves were found to be 20, 14, 12 and 17nm respectively. The BET surface areas calculated for CuO nanoparticles, nanotubes, nanoflowers and nanoleaves were found to be 38.87, 55.90, 65.34 and 46.88 m^2/g, respectively.

SEM and TEM analysis

From the Fig. 2 (a) SEM, (b) TEM, (c) SAED pattern (d) Histogram depicting the size distribution of CuO nanoparticle. The SEM of CuO shows a homogeneous distribution of particles of the prepared CuO. TEM images confirmed the particle nature of the sample with uniform size and shape. The corresponding Selected Area Electron Diffraction (SAED) pattern consists of bright rings and can be interpreted that nanoparticles are polycrystalline in nature.

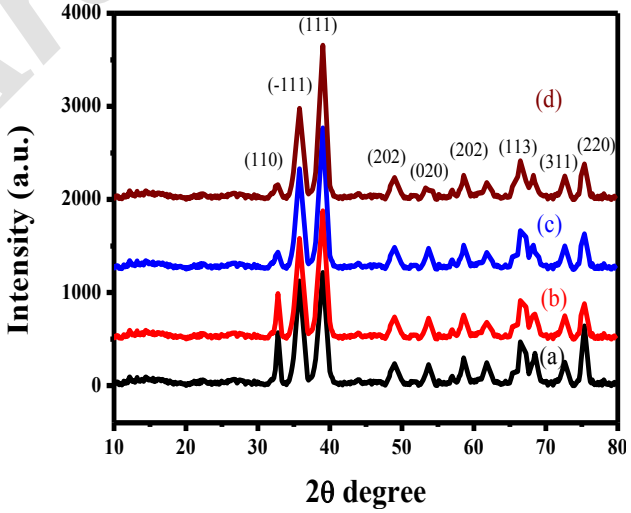

Fig. 1: XRD pattern of CuO (a)nano particles (b) nano leaves (c)nano tubes and (d) nano flowers.

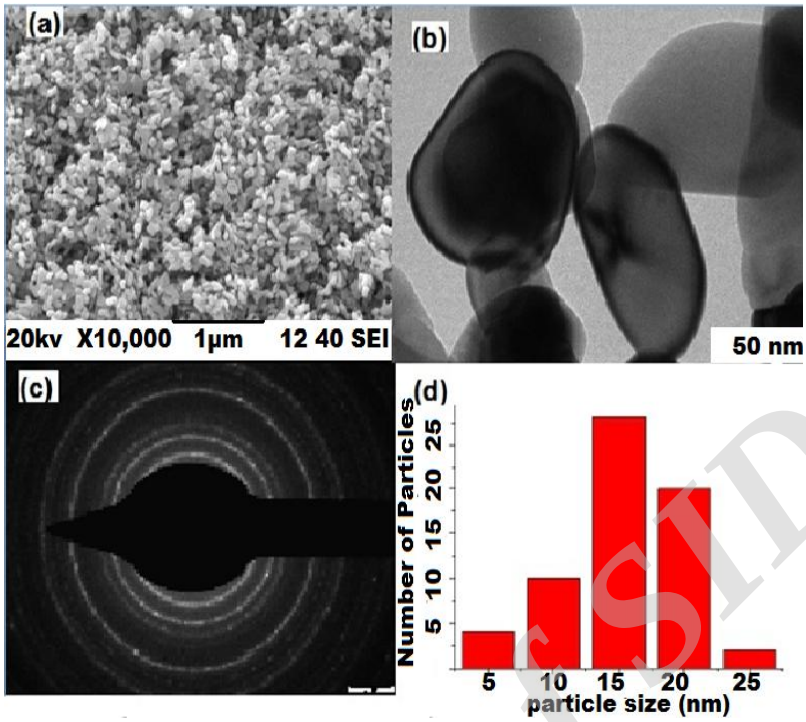

Fig. 2: (a) SEM (b) TEM (c) SAED pattern (d) Histogram depicting the size distribution of CuO nanoparticle.

Fig. 3 (a) SEM, (b) TEM, (c) SAED pattern, (d) Histogram depicting the size distribution of CuO nanotubes. The SEM image of CuO nanotubes, it is found that the surface of the nanotubes is not very smooth. Furthermore, the open tips indicate its hollow characteristics. TEM image also clearly shows the tube shape. Average diameters of open tips of these nanotubes are found to be in nanometer regime. SAED pattern reveals a polycrystalline nature, consisting of several nanocrystals. In addition to this, the rings consisting of the diffraction patterns are diffuse which suggests that there exists a preferential orientation among nanocrystals.

Fig. 4 (a) SEM, (b) TEM, (c) SAED pattern, (d) Histogram depicting the size distribution of CuO nanoflowers. TEM images show the flower-like morphology of prepared CuO, where these nanoflowers show uniform size and shape. A moderate alkali such as HMT and microwave irradiation plays an important role in the formation of these beautiful nanostructures. As a polar material, CuO might have been affected significantly by microwave irradiation.The applied microwave field induces a rotation of polarized dipole of polar materials, which can generate heat due to molecular inner friction. The presence of internal electric field, leads to orientation effects of dipolar molecules and hence reduce the activation energy [11]. The reduction in surface energy of the polar crystal may be the primary driving force for the nucleation, growth of the material and morphology evolution. The growth rate of different crystal planes determines the shape and structure of the crystal. Any change in the growth conditions alters the overall energy of crystal nuclei and hence the formation of different size and shape [12]. The TEM image of a single nanoflower composed of many petals. The SAED pattern obtained for these nanoflowers shows that the diffraction points are slightly stretched which indicates that the CuO nanoflowers are composed of nanocrystals that were assembled via oriented attachment process. Mechanisms of formation of CuO nanoflowers are believed to be as follows

$$\begin{aligned} HMT + 6H_2O &\rightarrow 4NH_3 + 6HCHO \\ NH_3 + H_2O &\rightarrow NH_4^+ + OH^- \\ Cu^{2+} + 2OH^- &\rightarrow CuO + H_2O \end{aligned} \quad (4)$$

Fig. 5 (a) SEM, (b) TEM, (c) SAED pattern, (d) Histogram depicting the size distribution of CuO nanoleaves. The surface morphology of synthesized CuO shows the long leaf-like morphology with the

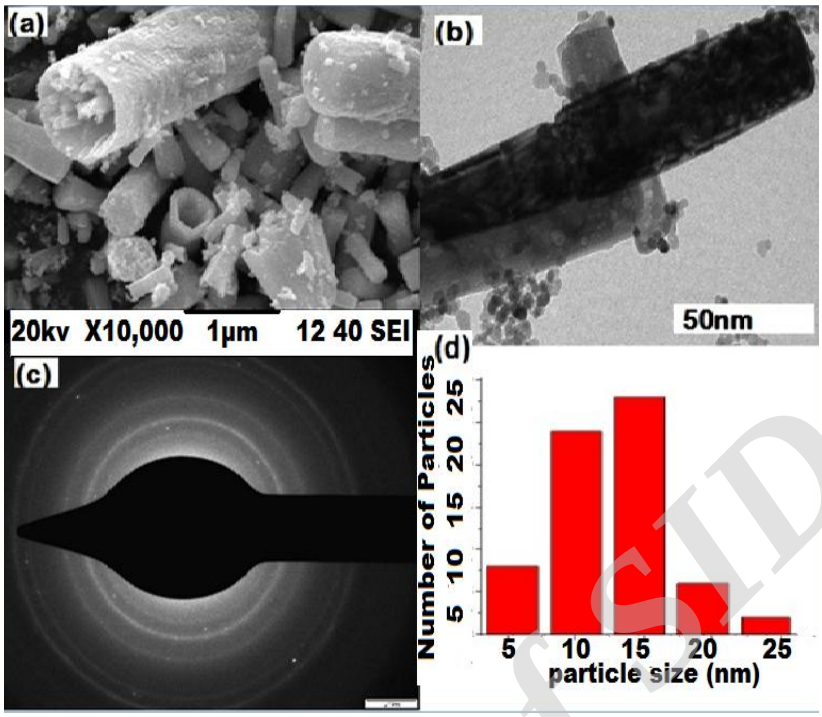

Fig. 3: (a) SEM (b) TEM (c) SAED pattern (d) Histogram depicting the size distribution of CuO nanotubes.

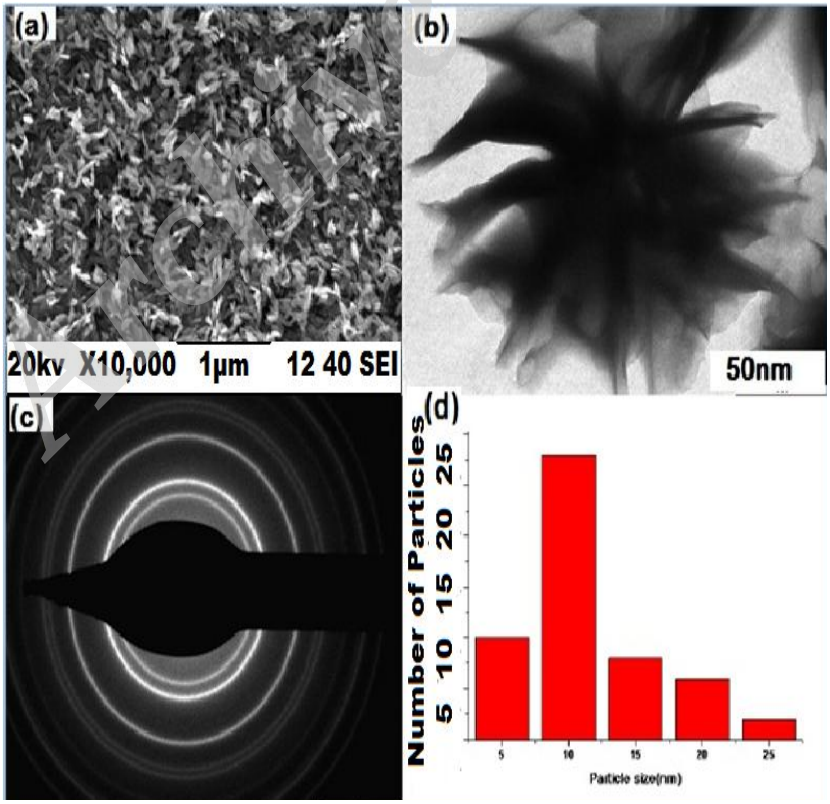

Fig. 4: (a) SEM (b) TEM (c) SAED pattern (d) Histogram depicting the size distribution of CuO nanoflowers.

wider center part and both sides having very sharp tips, similar to bamboo-leaves. In the presence of NaOH, the fast transformation results in a quick aggregation of the CuO nanoparticles to decrease the surface energy. TEM image also confirms the formation of an elongated shape. These elongated structures with an average diameter and length are also found to be in nanometer size. SAED pattern consists of bright rings and shows the polycrystalline nature of the synthesized nanoparticles.

The nature of the alkali plays an important role in the formation of these beautiful nanostructures. Usage of a moderate alkali such as HMT favors the growth of CuO in a 3D manner. The nanoparticle growth depends on the surface energy and consequently the differences of various surface energies lead to different types of morphology. In alkaline solution, adsorption of –OH ions on the surface of nanoparticles change their surface energy and hence –OH ion concentration might play a role in the aggregation mechanism. Here, a moderate alkali such as HMT prefers anisotropic growth in three dimensions. This occurs because the nanoparticles are self-assembled through an oriented attachment mechanism, where the individual particles align with respect to each other so that they share identical crystal faces. The driving force for this oriented attachment mechanism is the reduction of overall surface energy [13]. While using a strong alkali such as NaOH, the kinetics of transformation is very fast because Cu^{2+} ions are in the form of tetrahydroxocuprate (II) anions, which are stabilized by a strong Jahn-Teller effect. This may decrease the probability of oriented attachment growth [14].

FTIR and UV-Visible spectroscopic studies

FTIR analysis is carried out to identify the possible bio-molecule responsible for capping and efficient stabilization of the nano CuO synthesized using pomegranate. Fig. 6 shows the FTIR spectra of pomegranate fruit juice and nano CuO. The absorption bands at 3421 cm^{-1}, 2360 cm^{-1}, 1630 cm^{-1} and 1080 cm^{-1} in the spectrum of pg correspond to

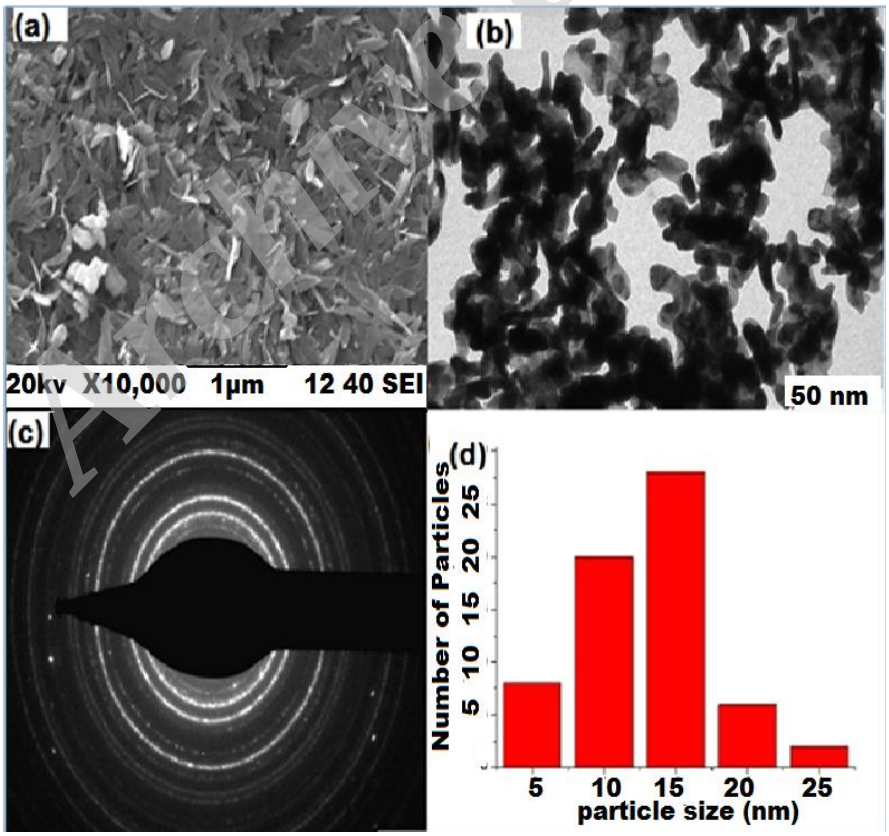

Fig. 5: (a) SEM (b) TEM (c) SAED pattern (d) Histogram depicting the size distribution of CuO nanoleaves.

the O-H stretching vibration of phenolic hydroxyls, stretching vibrations of NH^{2+} and NH^{3+} in protein/ peptide bonds, carbonyl stretching in proteins and C-OH vibrations, respectively, of proteins present in pg extract. A relative decrease in the intensity of phenolic hydroxyl stretching band in the spectrum of pg fruit extract after the reaction indicates the partial role of phenolic hydroxyls in the reduction mechanism and forming quinones. The FTIR spectrum of nano CuO shows bands at around 601,508 and 487 cm^{-1}, which can be assigned to the vibrations of Cu(II)-O bonds. The broad absorption peak at around 3430cm^{-1} is caused by the –OH bending vibrations of adsorbed water molecules since the nanocrystalline materials exhibit a high surface to volume ratio and thus absorbs moisture. The complete disappearance of the NH^{2+} and NH^{3+} stretching vibrations in the FTIR spectra of CuO can be attributed to the breaking of amino acid residues of proteins during the reaction. A similar mechanism involving the role of phenolic hydroxyls and proteins in the reduction and stabilization of individual nanomaterials have been reported previously [15].

The UV-Visible absorption spectra of the samples are taken in the wavelength range of 200 to 800 nm. Fig. 7 shows the UV-Visible spectra of CuO (a) nanoparticles (b) nanotubes (c) nano leaves (d) nanoflowers. In the absorption spectra of the synthesized CuO, the absorption edge is blue shifted to shorter wavelength with changed morphology. The observed spectrum and estimated band gap for the morphology of CuO reveal that in addition to size, morphology also affects the band gap of CuO structures. The band gaps (obtained from Tauc's plots) of the CuO nanoparticles, nanotubes, nano leaves, and nanoflowers were found to be as 2, 2.2, 2.9 and 3.1 eV respectively. In the case of CuO nanoflowers and nanotubes observed blue shift can be ascribed to the strong Quantum Confinement effect, resulting in a larger band gap [16].

Photoluminescence (PL) Spectral Analysis

Fig. 8 shows the PL spectra of (a) nanoparticles (b) nano leaves (c) nanotubes (d) nanoflowers in a wavelength range of 350 to 650 nm. PL spectra of all samples show three main broad emission bands centered at~318, ~525, and ~615 nm. The PL peak at ~318 nm is due to the band-edge emission of CuO nanostructures. The three-strong emission peaks located at 440, 463, and 505 nm are due to the band edge emission from the new sublevels or maybe due to the defects present in the CuO nanostructures. The emission bands extending from 585 to 625 nm correspond to deep level defects of CuO. There are slight changes in intensities and wavelengths of the PL peaks among the different samples of CuO. The peaks of CuO nanoflowers are blue shifted compared to nanoparticles. From this, it is clear that the PL properties of CuO nanostructures can be controlled by their shape, dimension, and morphology. Quantum chemical effect and specific surface effect are the two most reported mechanisms, which can result in the blue shift and red shift of the PL peak [17]. There are several reports that the photoluminescence properties of CuO nanostructures have been controlled by their shape, dimension, and morphology [18].

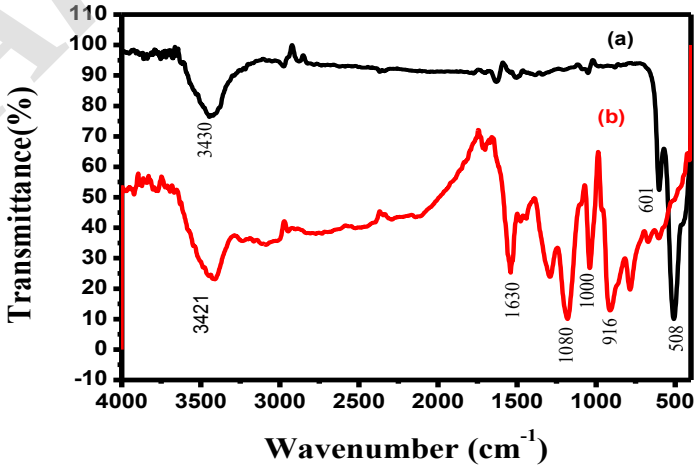

Fig. 6: FTIR Spectra of (a) CuO (b) Pomegranate fruit extract.

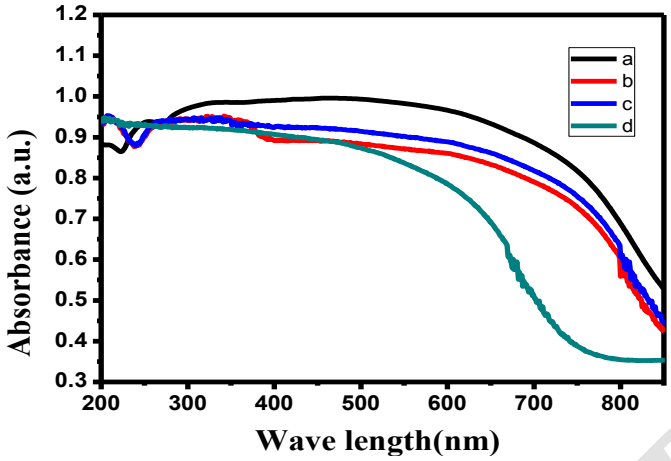

Fig. 7: UV-Visible spectra of CuO (a) nano particles (b) nano tubes (c) nano leaves (d) nano flowers.

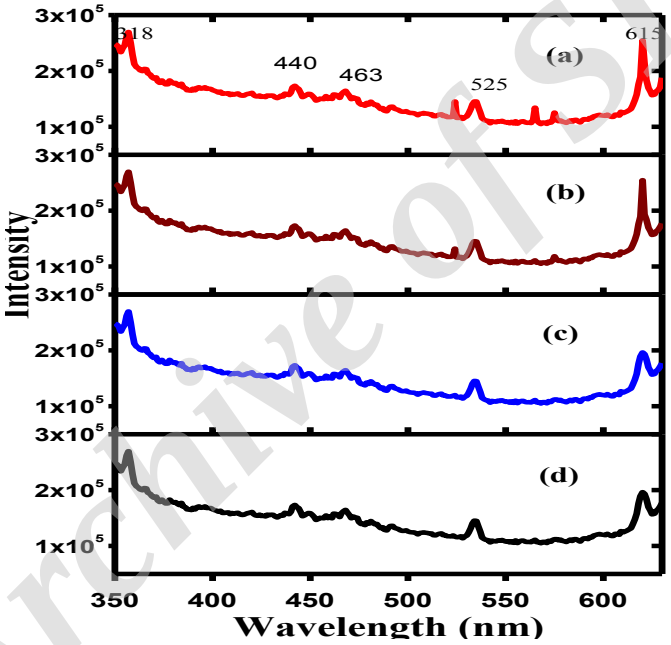

Fig. 8: The PL spectra of (a)nano particles (b) nano leaves (c)nano tubes (d) nano flowers.

Photo Catalytic Studies

Fig. 9 shows the time-dependent absorption spectra of malachite green dye under UV irradiation with (a) CuO nanoleaves (b) particles (c) flowers (d) tubes. Experimental results reveal that copper oxide nanostructures degrade malachite green more effectively than congo red. The percentage degradation of malachite green was highest with flower type CuO nanomaterials (95%). The photocatalytic degradation efficiency of copper oxide particles was found to be 72%, for tube type it was 88% and for the leaves type, it was 82% after 150 minutes of UV irradiation. Similar results obtained for the photocatalytic degradation of congo red.

Fig. 10 shows the time-dependent absorption spectra of congo red dye under UV irradiation with (a) CuO nanoleaves, (b) particles (c) flowers (d) tubes. Here the degradation efficiency for copper oxide particle type was found to be 62%, for nanotubes it was 83%, for nano leaves 80% and for the flower type, it was 91% after 150 minutes of UV irradiation.

From experimental results, shape factor seems

to be of overriding importance to degradation efficiency. As the way that a crystal is organized and structured will determine the behavior of the atoms that constitute the crystal and catalytic activity depends upon the surface structure of a crystal. Zhang et al reported that (111) facet are more active due to dangling bonds, while other facets have saturated chemical bonds and no dangling bonds exist. So the copper oxides with dominant (111) facet have higher adsorption and photocatalytic activity than those with other dominant surfaces [19]. The flower-like CuO composed of tiny crystals with dominant (111) facet, shows comparatively higher absorbance, higher surface area, and wider band gap. Hence exhibit much higher degradation efficiency. The photocatalytic degradation follows the order CuO nanoflowers > nanotubes > nanoleaves > nanoparticles. The lowest photocatalytic activity of spherical CuO can be attributed to their lesser surface area.

Many previous studies on the degradation of dyes using CuO emphasize the importance of H_2O_2 in the process [20-24]. But in the present study, the prepared nanostructures of CuO show good degradation efficiency without using H_2O_2. One of the important parameters which affect the degradation of organic dyes is the presence of oxygen atoms on the surface of a photocatalyst [25]. The prepared CuO nanomaterials have a number of surface oxygen atoms in different morphological forms and hence different activity.

The relatively high band gap in the synthesized

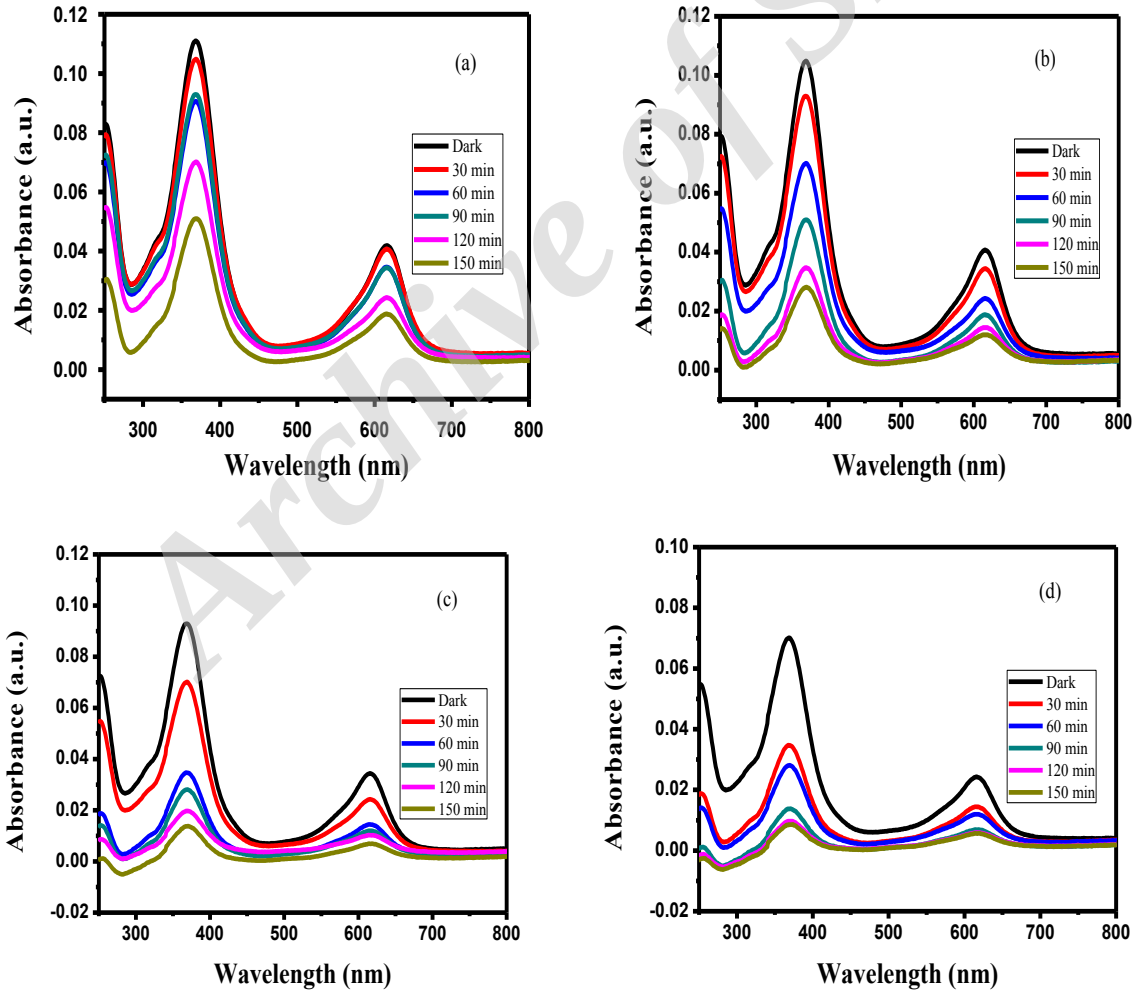

Fig. 9: Time dependent absorption spectra of malachite green dye under UV irradiation with (a) CuO nanoleaves (b) particles (c) flowers (d) tubes.

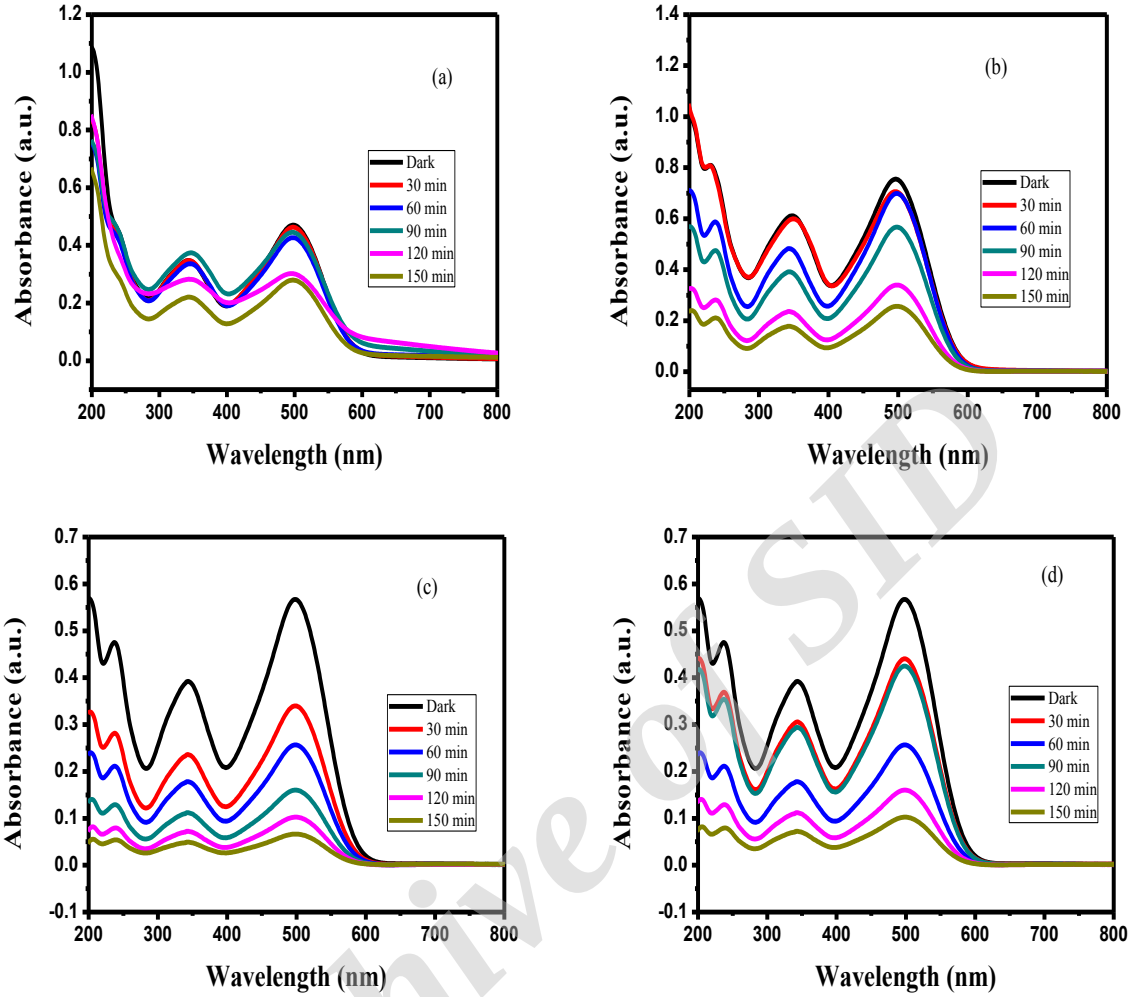

Fig. 10: Time dependent absorption spectra of congo red dye under UV irradiation with (a) CuO nanoleaves, (b)particles (c) flowers (d)tubes.

CuO nanomaterials is expected to prevent the recombination of photogenerated electrons and holes, which are responsible for the production of reactive species ($OH^{\bullet}$ and $O_2^{\bullet -}$) involved in the degradation process [26]. The nano CuO with flower-like morphology was found to have maximum band gap values and hence its higher activity can be accounted. Further, its high surface area and structural parameters might have contributed to its efficiency.

Antimicrobial studies

The synthesized nanostructures of CuO were evaluated for their antimicrobial properties towards bacterial and fungal strains. Fig. 11. Zone of inhibition of CuO nanostructures (a-CuO nanoflowers, b-tubes, leaves, and d-particles), are against microbial strains. The antimicrobial studies showed that different morphologies of CuO nanostructures demonstrate different antimicrobial activities against microbial strains. It is clear from Table 1, those nanoflowers and nanotubes have a higher antimicrobial activity than nanoleaves and nanoparticles, because of their larger surface area. The unique surface features of the nanoflowers and tubes were able to induce more surface related phenomena. This particle generates more ROS on their surface which get attached to the bacterial cells, and in turn, provoke an enhancement of the intracellular oxidative stress facilitating the higher antimicrobial activity [27].

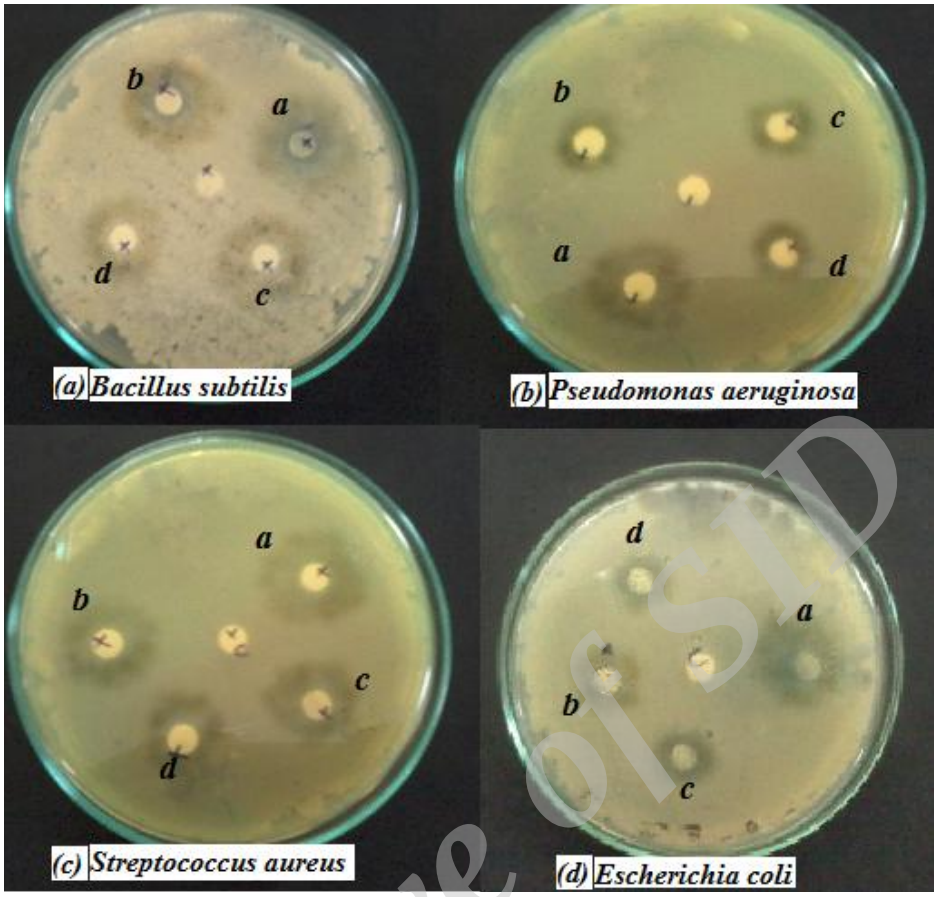

Fig. 11: Zone of inhibition of CuO nano structures a- CuO nanoflowers, b-tubes , c-leaves d-particles against microbial strains.

Table 1: Comparison of antimicrobial activities of CuO nanostructures.

CuO nano structures	Zone of inhibition(mm)					
	E. coli	*Pseudomonas aeruginosa*	*Bacillus subtilis*	*Streptococcus aureus*	*Penicillium chrysogenum*	*Aspergillus flavus*
Nano particles	4	5	7	6	6	9
Nano leaves	6	5	10	8	9	8
Nano tubes	6	9	12	11	8	10
Nano flowers	9	11	17	14	11	13

Truncated triangular silver nanoplates with exposed (111) lattice plane displayed strongest biocidal action compared with spheres and rod-shaped nanoparticles [28]. Similar results were obtained for our synthesized CuO nanostructures also. The nanostructures with exposed (111) lattice planes (nanoflowers and nanotubes) showed higher antimicrobial activity compared to nanoleaves and nanoparticles. This is due to the higher chemical reactivity of exposed (111) lattice planes. The complicated atomic stacking of (111) facets allows the O atoms at the surface be more polarized than the other facets [29]. This phenomenon leads to a higher chemical activity of the (111) facets and enhanced antimicrobial activity of CuO nanoflowers.

CONCLUSION

CuO nanostructures such as nanoparticles, nanotubes, nanoleaves, and nanoflowers are successfully synthesized. The nanostructures are characterized by XRD, SEM, and TEM. It was found that choice of alkali offers an excellent tool for the design of nanomaterials. Oriented attachment growth was observed which leads to the formation of three-dimensional on using moderate alkali solution. The potential application of these nanostructures for the degradation of Congo red and Malachite Green was examined and the observed results show the better photocatalytic efficiency of CuO nanoflowers compared to the other morphologies. The elevated photocatalytic efficiency of CuO nanoflowers is due to its higher surface area and oxygen vacancies accompanied by large energy defects. CuO nanostructures show excellent bactericidal potential against both gram-positive and gram-negative bacterial strains. In this case, the higher antibacterial activity is for a peculiar flower-like structure because of its higher surface area compared to conventional CuO nanostructures.

ACKNOWLEDGMENTS

The authors wish to acknowledge CSIR, New Delhi for financial assistance in the form of SRF, SAIF Mumbai for TEM analysis and STIC Cochin for other instrumental analysis.

CONFLICT OF INTEREST

The authors declare that there is no conflict of interests regarding the publication of this manuscript.

REFERENCES

[1] Nasser M. H., Mohamed S. Z., (2012), Polymethacrylic acid as a new precursor of CuO nanoparticles. *J. Molec. Struc.* 1027: 128-132.

[2] Asha R., Rejani A., Beena B, (2014), Synthesis, characterization and antimicrobial properties of CuO nanoparticles against gram-positive and gram-negative bacterial strains. *Int. J. Nano Dimens.* 5: 519-524.

[3] Wu-Wu Li., Ying Guo., Wei-Hong Z., (2017), A porous Cu(II) metal-organic framework: Synthesis, crystal structure and gas adsorption properties. *J. Molec. Struct.* 1143: 20-22.

[4] Rehman S., Mumtaz A., Hasanain S. K., (2010), Size effect on the magnetic and optical properties of CuO nanoparticles. *J. Nano Part. Res.* 13: 2497-2507.

[5] Zhou L. P., Wang B. X., Peng X. F., Du X. Z., Yang Y. P., (2010), On the specific heat capacity of CuO nanofluid. *Adv. Mech. Eng.* 2010: 1-4.

[6] Wang S. B. B., Hsiao CH. H., Chang S. J. J., Lam K. T. T., Wen K. H. H., Hung S. C. C., (2011), A CuO nanowire infrared photodetector. *Sensor Actuat A.: Phys*. 171: 207-211.

[7] Zhang X., Shi W., Zhu J., Kharistal D., Zhao W., Lalia B., (2011), High-power and high-energy-density flexible pseudocapacitor electrodes made from porous CuO nanobelts and single-walled carbon nanotubes. *ACS Nano*. 5: 13-9.

[8] Asha R., Rejani B., (2015), CuO/polypyrrole nanocomposites as a marker of toxic lead ions for ecological remediation in contrast with CuO and polypyrrole. *Main Group Met. Chem.* 38: 133-143.

[9] Yu X-Y., Xu R-X., Gao C., Luo T., Jia Y., Liu J-H., (2012), Novel 3D hierarchical cotton-candy-like CuO: surfactant-free solvothermal synthesis and application in As(III) removal. *ACS Appl. Mater. Interfaces*. 4: 1954-1962.

[10] Khojier K., Behju A., (2012), Annealing temperature effect on nanostructure and phase transition of copper oxide thin films. *Int. J. Nano Dimens.* 2: 185-190.

[11] Asha R., Rejani P., ShanavasKhan J., Beena B., (2016), Effect of annealing on the spectral and optical characteristics of nano ZnO: Evaluation of adsorption of toxic metal ions from industrial wastewater. *Ecotoxicol. Environ. Safety.* 133: 457-465.

[12] Aghabeygi Sh., Zare-Dehnavi B., (2015), Sono-Synthesis and characterization of ZrO_2/ZnO nanocomposite, composition effect on enhancing of photocatalytic properties. *Int. J. Nano Dimens.* 6: 297-304.

[13] Cudennec Y., Lecerf A., (2003), The transformation of $Cu(OH)_2$ into CuO. *Solid State Sci.* 5: 1471-1474.

[14] Kazeminezhad I., Sadollahkhani A., (2014), Photocatalytic degradation of Eriochrome black-T dye using ZnO nanoparticles. *Mater. Lett.* 120: 267-270.

[15] Meena K. M., John J., Daizy P., (2015), Green synthesis and applications of Au-Ag bimetallic nanoparticles. Spectrochim. *Acta Part A: Molec. Biomolec. Spec.* 37: 185-192.

[16] Rehman S, Mumtaz H., (2010), Size effect on the magnetic and optical properties of CuO nanoparticles. *J. Nano Part. Res.*13: 2497-507.

[17] Lin H-H., (2004), Characterizing well-ordered CuO nanofibers synthesized through gas-solid reactions. *J. Appl. Phys.* 95: 5889-5895.

[18] Al-Gaashani R., Radman S., Tabet N., Razak D., (2011), Synthesis and optical properties of CuO nanostructures obtained via a novel thermal decomposition method. *J. Alloys and Comp.* 509: 8761-869.

[19] Zhang Y., Deng B., Zhang T. R., Gao D. M., Xu A. W., (2010), Shape effects of Cu_2O polyhedral microcrystals on photocatalytic activity. *J. Phys. Chem. C.* 114: 5073-5079.

[20] Miyauchi M., Nakajima A., Watanabe T., Hashimoto K., (2002), Photocatalysis and photoinduced hydrophilicity of various metal oxide thin films. *Chem Mater*. 14: 2812-2816.

[21] Yu H., Yu J., Liu S., Mann S., (2007), Template-free hydrothermal synthesis of CuO/Cu_2O composite hollow microspheres. *Chem Mater*. 1943: 27-34.

[22] Yang He., (2011), Fine tuning of the morphology of copper oxide nanostructures and their application in ambient degradation of methylene blue. *J. Colloid Interf. Sci*. 355: 15-22.

[23] Srivastava R., Anu Prathap M. U., Kore R., (2011), Morphologically controlled synthesis of copper oxides and their catalytic applications in the synthesis of propargylamine and oxidative degradation of methylene blue. *Colloids Surf. Physicochem. Eng. Aspects*. 392: 271-282.

[24] Xu H., Zhu G., Zheng D., Xi C., Xu X., Shen X., (2012), Porous

CuO superstructure: Precursor-mediated fabrication, gas sensing and photocatalytic properties. *J. Colloid Interf. Sci.* 383: 75-81.

[25] Zaman S., Zainelabdin A., Amin G., Nur O., Willander M., (2012), The efficient catalytic effect of CuO nanostructures on the degradation of organic dyes. *J. Phys. Chem. Solids.* 73: 1320-1325.

[26] Navid A., Aberoomand P., (2017), Synthesis of ZnO-nanoparticles by microwave assisted sol-gel method and its role in the photocatalytic degradation of food dye Tartrazine (Acid Yellow 23). *Int. J. Nano Dimens*. 8: 241-249.

[27] Saeed F., Bahram A., Abdelnassar M., (2017), Low-cost and eco-friendly photo-synthesis of Silver nanoparticles by using grapes fruit extract and study of antibacterial and catalytic effects. *Int. J. Nano Dimens*. 8: 49-60.

[28] Pal S., Tak Y. K., Song J. M., (2007), Does the antibacterial activity of silver nanoparticles depend on the shape of the nanoparticle? A study of the gram-negative bacterium Escherichia coli. *Appl. Environm. Microbiol.* 27: 1712-1720.

[29] Kim K. J., Sung W. S., Moon S. K., Choi J. S., Kim J. G., Lee D. G., (2008), Antifungal effect of silver nanoparticles on dermatophytes. *J. Microbiol. Biotechnol.* 18: 1482-1484.